ACS APPLIED MATERIALS & INTERFACES

Research Article

www.acsami.org

Mechanically Tough, Electrically Conductive Polyethylene Oxide Nanofiber Web Incorporating DNA-Wrapped Double-Walled Carbon Nanotubes

Jin Hee Kim,[†] Masakazu Kataoka,[†] Yong Chae Jung,[‡] Yong-Il Ko,[†] Kazunori Fujisawa,[†] Takuya Hayashi,[†] Yoong Ahm Kim,*[,†] and Morinobu Endo[§]

[†]Faculty of Engineering, Shinshu University, 4-17-1 Wakasato, Nagano 380-8553, Japan

[‡]Korea Institute of Science and Technology (KIST), Eunhari san 101, Bongdong-eup, Wanju-gun, Jeonbuk 565-905, Korea

[§]Research Center for Exotic Nanocarbons (JST), Shinshu University, 4-17-1 Wakasato, Nagano 380-8553, Japan

ABSTRACT: Electrospun biopolymer-derived nanofiber webs are promising scaffolds for growing tissue and cells. However, the webs are mechanically weak and electrically insulating. We have synthesized a polyethylene oxide (PEO) nanofiber web that is pliable, tough, and electrically conductive, by incorporating optically active, DNA-wrapped, double-walled carbon nanotubes. The nanotubes were individually trapped along the length of the PEO nanofiber and acted as mechanically reinforcing filler and an electrical conductor.

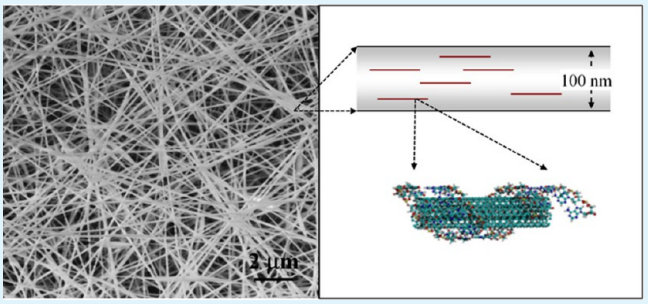

KEYWORDS: *electrospinning, PEO, carbon nanotube, nanofiber, mechanical strength, electrical conductivity*

INTRODUCTION

Electrospinning is a fast, simple technique that can be used to fabricate nanofiber webs from a variety of polymers.[1,2] Electrospun fibers exhibit a variety of desirable properties, such as nanoscale diameter, highly accessible surface area, tunable porosity, versatile surface properties, and thin web morphology. They are promising materials for artificial organs, for cell and tissue scaffolds, and for drug and gene delivery.[3−13] However, the practical applications of nanofiber webs have been limited, because the biopolymers are electrically insulating and mechanically weak.

These limitations can be addressed by using one-dimensional carbon nanotubes as a multifunctional filler for polymeric nanofibers, because carbon nanotubes are electrically conductive, optically active, mechanically strong, and have a sufficiently small diameter.[14] Carbon nanotubes, disentangled by using sodium dodecyl sulfate, poly(vinyl pyrrolidone), and gum arabic, have been successfully embedded in electrospun polymeric nanofibers.[15,16] However, the electrical and mechanical properties of the nanofiber web were not investigated, and toxic surfactants cannot be used to prepare functional tissue engineering scaffolds. Herein, biocompatible DNA molecule is chosen in our study, because DNA was identified as a powerful dispersing agent to disentangle strongly bundled metallic/semiconducting nanotubes and to separate single-chirality nanotubes in an aqueous solution, because of DNA molecules' ability to wrap around the sidewalls of carbon nanotubes.[17−28] DNA is abundant and easier to handle than protein, because of its high thermal stability, and, moreover, DNA can also be used to induce cells to divide. Therefore, DNA molecules have been incorporated in electrospun biopolymeric nanofibers.[29,30]

Herein, we have developed a method of fabricating a polyethylene oxide (PEO) nanofiber web, which is thin, tough, electrically conductive, and optically active, by incorporating DNA-wrapped carbon nanotubes and DNA into the biopolymeric nanofibers. The DNA-wrapped nanotubes acted as a mechanical reinforcing filler and an electrical conductor. Bright optical signals from the inner tubes of the double-walled carbon nanotubes (DWNTs) indicated that the DWNTs were trapped in the PEO nanofiber web. Our PEO nanofiber web with tunable porosity could be used to fabricate a spatially and temporally controlled scaffold for growing cells.

EXPERIMENTAL SECTION

Dispersion of Double-Walled Carbon Nanotubes. The highly pure crystalline DWNTs were prepared by chemical vapor deposition followed by oxidative purification.[31,32] Salmon DNA (300 base, Maruha Nichiro) was used as the starting material. The homogeneously dispersed (i.e., individualized) DWNT solutions were prepared as previously reported.[33] The base pair of dsDNA after sonication was found to be ca. 150−200. We found a saturated fragmentation of the DNA under our sonication conditions. The DWNT (2 mg) were dispersed in double-stranded DNA (dsDNA) solution (10 mL) by sonication for 1 h at 4 °C. The amount of the individually dispersed tubes in the supernatant was found to be ca. 10%, with regard to the starting DWNT sample.[34] Then, we used a

Received: January 9, 2013
Accepted: April 18, 2013
Published: April 18, 2013

Qubit fluorometer to measure the adsorbed DNA to DWNTs in the supernatant by removing any free DNA. The amount of the adsorbed DNA on DWNTs was found to be ca. 12.1 μg/mL. The suspensions were ultracentrifuged (150 000 g) to obtain the individually dispersed DWNTs. The dispersion of the DWNTs in the DNA solution was confirmed by the ultraviolet−visible light (UV-vis) absorption spectra (SolidSpec-3700, Shimadzu) and photoluminescence maps (NIR-PL system, Shimadzu). Raman/fluorescence spectra were obtained at an excitation wavelength of 785 nm using a Raman spectrophotometer (inVia, Reinshaw) fitted with a macroscopic sampling kit.

Preparation of PEO and PEO/DNA Solution. PEO (7 wt %, MW = 300 000, Aldrich) was dissolved in distilled water. A DNA (7 wt %) or DNA-dispersed DWNT solution was added to the PEO solution at different blending ratios (PEO/DNA = 100/0, 90/10, 80/20, 70/30, 60/40, 50/50, 40/60, 30/70, 20/80, and 10/90). A DNA-dispersed DWNT solution (1% or 5%) was added to the PEO/DNA solution.

Nanofiber Formation Using the Electrospinning System. The PEO/DNA solution was transferred into a 5-mL syringe with a capillary tip of 0.5 mm in diameter. The electrospinning was carried using standard equipment, with a voltage of 10−15 kV, a flow rate of 0.3−0.5 mL/h, and a tip-to-collector distance of 8−12 cm. The electrospun fibers were collected as a thin web by a metal drum wrapped in aluminum foil, rotating at ∼50 rpm.

Analysis of Electrospun Nanofiber Web. The macromorphology of the nanofiber web was observed by field-emission scanning electron microscopy (FE-SEM; Model JSM-7000F, JEOL). The Raman map of the electrospun nanofiber web using a 532-nm laser line was obtained using a Raman microscope (inVia, Reinshaw). Electrical conductivity measurements were carried out using the 1M6exZAHNER electric analyzer. A standard four-probe method was used to measure the electrical conductivity for all of the composites films at ambient conditions of 25 °C. The mechanical properties of the nanofiber web samples (60 mm × 10 mm × 0.50 mm) were evaluated at room temperature, according to the ASTM D638 test method using a tensile tester (Tensilon RTC, A&D), with a gauge length of 25 mm, crosshead speed of 10 mm/min, and load cell of 2.5 kN. A standard four-probe method was used to measure the electrical conductivity of the composite films (1M6ex, Zahner-Elektrik).

RESULTS AND DISCUSSION

DWNTs were used instead of single-walled carbon nanotubes (SWNTs), because strong optical signals were observed from the inner nanotubes, since the outer nanotubes protected the inner nanotubes from physical and chemical attack.[35−37] High-purity DWNTs, prepared by catalytic CVD and oxidative purification,[31,32] were used as a reinforcing filler for the nanofibers. Figures 1a and 1b show that the nanotubes were tightly bundled and stacked in a regular hexagonal arrangement (inset, Figure 1b).[31] In addition, the high crystallinity of the DWNTs was confirmed by the absence of the D-band from the Raman spectra, using a 532-nm laser line (Figure 1c).[32] An opaque DWNT dispersion in an aqueous solution of DNA was obtained by sonication and ultracentrifugation (Figure 1d). The strong van der Waals interaction between the DNA and the DWNTs caused the DNA to wrap around the DWNT sidewalls, and thus allowed the DWNTs to disperse (inset, Figure 1d). The DWNT dispersion was optically characterized. Sharp optical absorption peaks in the UV absorption spectrum (Figure 1d) and several strong photoluminescence peaks in the PL map (Figure 1e) showed that the DWNTs were individually dispersed in the aqueous DNA solution.

The polymer matrix was PEO, which was selected because of its high biocompatibility and nonfouling properties. PEO is soluble in water, but it does not have the ability to disperse carbon nanotubes, because of its structure ($HO-CH_2-(CH_2-O-CH_2)_n-CH_2-OH$). For this reason, the effects of the PEO

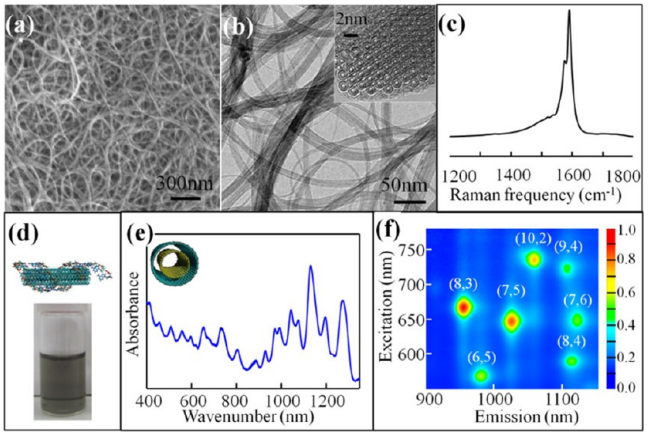

Figure 1. (a) SEM and (b) TEM images of catalytically grown DWNTs. Inset in panel (b) is a cross-sectional TEM image showing the hexagonally packed structure. (c) Raman spectrum of the DWNT sample using a 532-nm laser line. (d) Image showing the opaque dsDNA-dispersed DWNT solution; the inset is a schematic model of dsDNA-wrapped DWNT. (e) UV−visible absorption spectra and (f) photoluminescence map of the dsDNA-dispersed DWNT suspension at pH 8.0. The sharp absorption peaks and bright photoluminescence spots indicate that the tubes were individually dispersed in the aqueous solution.

molecules on the stability and optical properties of the DNA-dispersed DWNT solution were examined. A PEO solution (1 wt %) was added to a DNA-dispersed DWNT solution and gently sonicated for 10 min. There was no visible change in the appearance of the nanotube solution (see inset, Figure 2). However, the Raman/fluorescence spectra of the DNA-dispersed DWNT solution changed following the addition of PEO. Figure 2a shows the low-frequency Raman spectra of both solutions. Three radial breathing modes (RBMs), which correspond to a coherent vibration of the carbon atoms normal to the tube axis, were observed below 500 cm^{-1}.[38] The RBM below 200 cm^{-1} was assigned to the outer metallic tubes, and the two RBMs above 200 cm^{-1} were assigned to the semiconducting inner tubes. The largely depressed outer tubes can be explained by the direct charge transfer from DNA to the metallic outer tubes.[33] The intensity of the RBM at 265 cm^{-1} in the DNA-dispersed solution was inversely proportional to the degree of dispersion of the tubes in the solution.[33] Thus, the increase in the intensity of the RBM at 265 cm^{-1} when the PEO solution was added indicated that the degree of dispersion decreased, because the PEO molecules weakened the binding of the DNA molecules to the surface of tubes. The high-frequency Raman spectra (Figure 2b) contained a strong G-band (E_{2g2} mode) at 1590 cm^{-1}, and a G′-band at ∼2700 cm^{-1}.[38] The strong luminescent peaks were assigned to the (6,4), (9,1), (8,3), (6,5), and (7,5) DWNT inner tubes, which indicates that the tubes were individually dispersed.[33,39] No significant change in the frequencies of the G and G′ bands or in the positions of the luminescent peaks was observed when PEO was added. However, the intensity of the luminescent peaks decreased, indicating that the degree of dispersion of tubes in solution decreased.

PEO/DNA solutions with different blending ratios were electrospun into nanofiber webs. Long nanofibers were obtained from the PEO/DNA solutions with blending ratios of 70/30 and 80/20, which is consistent with previously published data (see Figures 3a and 3b).[29,30] However, the

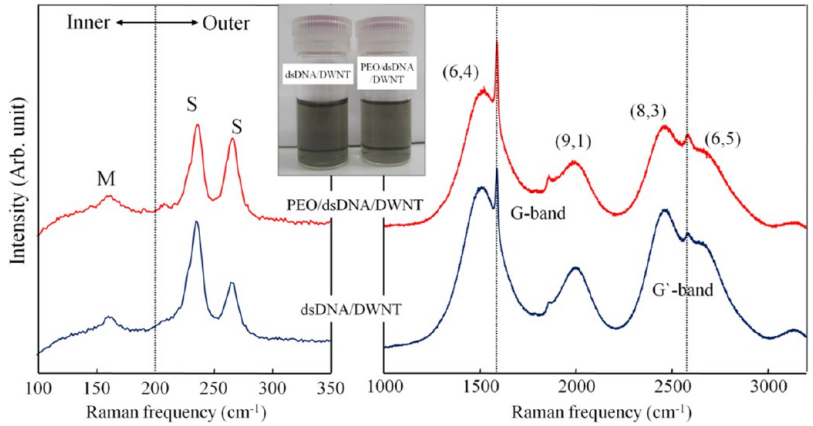

Figure 2. Raman/fluorescence spectra taken with a 785-nm laser line of the DNA-dispersed DWNT solution and the DNA-dispersed DWNT solution with PEO. The solutions appear the same to the naked eye; however, the intensity of the luminescent peaks decreased, which shows that the dispersion was reduced by adding PEO.

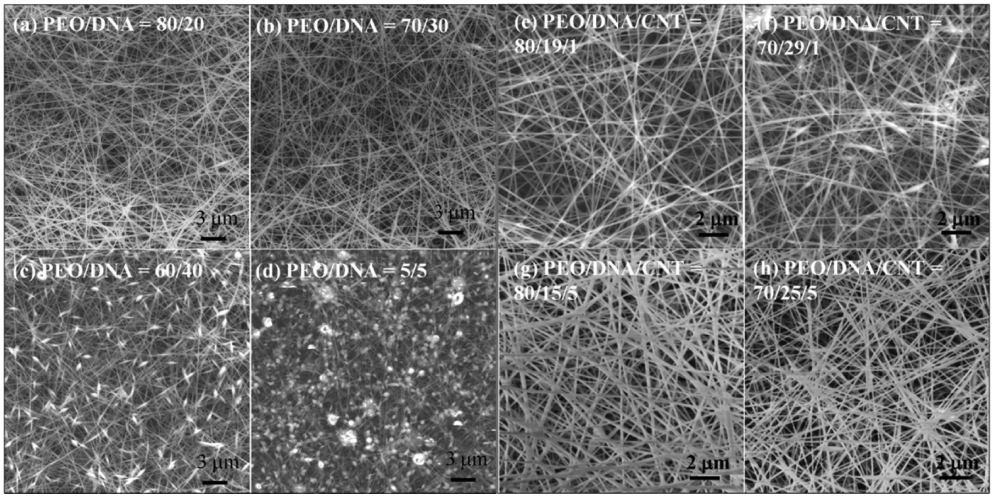

Figure 3. FE-SEM images of (a–d) the DNA-added PEO nanofiber web at different blending ratios and (e–h) the DNA-dispersed DWNT PEO nanofiber web containing (e, f) 1% DNA-dispersed DWNTs (panels (e) and (f)) and 5% DNA-dispersed DWNTs (panels (g) and (h)).

morphology of the electrospun material changed from fibers to beads as the fraction of DNA increased (see Figures 3c and 3d). This morphological change can be explained by the low spinnability of DNA solution. In addition, electrospinning PEO/DNA solutions with blending ratios of 80/20 and 70/30, which contained DNA-dispersed DWNT suspensions (1% or 5%), produced a white web (see Figures 3e–h) consisting of long, homogeneous nanofibers with a diameter of <100 nm. The miscibility of PEO and DNA in the electrospun nanofiber was characterized using low-resolution TEM. The absence of component separation indicates the phase miscibility of PEO/DNA was good (see Figure 4a). The high-resolution TEM images showed that the individual long carbon nanotubes were aligned along the length of the nanofiber (Figure 4b). SEM images were also obtained after the electrospun nanofiber web was washed with distilled water in order to remove the PEO matrix and verify that the DNA-wrapped nanotubes were trapped in the electrospun nanofiber (Figure 4c). Very long fibrous materials were observed in the SEM images. The DNA and DNA-wrapped DWNTs trapped in the PEO nanofiber probably formed the long, curled fibrous material. In addition, Raman map images of G-band and RBM (Figure 4d) obtained using a 532-nm laser line confirmed that the DWNTs were trapped in the fibrous material. The intermittent bright spots showed that the optically active DWNTs were present in the fibrous material.

The effect of the DNA-wrapped DWNTs in the PEO nanofiber was verified by measuring the electrical conductivity of the nanofiber webs by the four probe method and their mechanical strength by tensile testing. Table 1 shows the relatively high electrical conductivity of the PEO/DNA nanofiber web, which suggests that DNA acts as an electrical path in the PEO nanofiber.[40] Electrospinning a PEO solution that contained 5% DWNTs that were individually dispersed with DNA produced nanofibers with a conductivity of 3.72×10^2 S/cm. Figure 5 shows the stress–strain curves of the various nanofiber webs that were prepared by electrospinning PEO, DNA/PEO, and PEO/DNA/DWNT solutions. The addition of the DNA-wrapped DWNTs increased the elastic modulus of the PEO nanofiber web by 5-fold and the tensile strength by 2-fold, compared with the pure PEO nanofiber web. The improvement in the modulus and the tensile strength can be explained by the high aspect ratio of the DNA-wrapped DWNTs aligned along the length of the PEO nanofibers and by the strong nanoscale interfacial interaction between DNA and PEO, respectively. Thus, individual DNA-wrapped DWNTs are

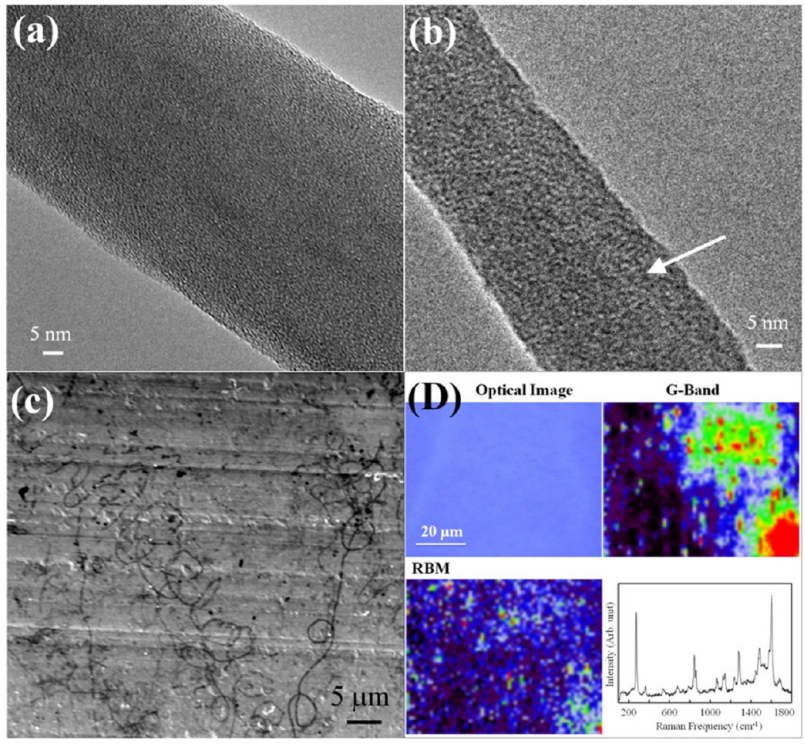

Figure 4. (a,b) TEM images of an individual electrospun nanofiber, and (c) FE-SEM image of an electrospun nanofiber washed in water. The long, curled fibrous materials were aggregated DNA-wrapped DWNTs. (d) Raman two-dimensional map images of G-band and RBM and its corresponding Raman spectrum of the electrospun nanofiber web using a 532-nm laser line.

Table 1. Electrical Conductivity of the PEO/DNA and PEO/DNA/DWNT Nanofiber Webs

Average Electrical Conductivity (S/cm)		
PEO/DNA	PEO/DNA/DWNT1%	PEO/DNA/DWNT5%
2.54×10^{-4}	7.65×10^{-2}	3.72×10^{2}

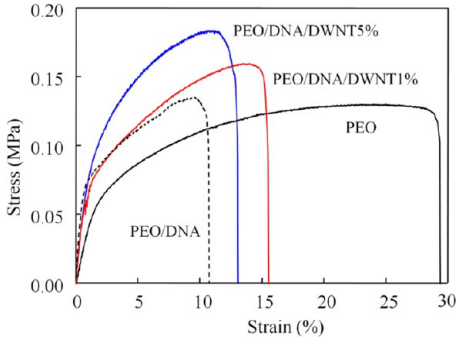

Figure 5. Stress−strain curves of nanofiber webs containing only PEO, DNA and PEO, and DNA-wrapped DWNT and PEO. A 5-fold increase in the modulus and a 2-fold increase in the tensile strength of the PEO nanofiber web were achieved by adding individually DNA-dispersed DWNTs.

probably present in the PEO nanofiber along the length of the fiber, and DNA molecules act as a buffer-like interphase between the DWNTs and PEO molecules.

CONCLUSIONS

We have successfully fabricated a web of long, homogeneous nanofibers by electrospinning PEO solution containing DNA-wrapped DWNTs. Strong optical signals coming from the inner tubes of the DWNT showed that the DWNTs were individually dispersed in the DNA solution. In addition, the homogeneous coating of the DNA-wrapped DWNTs with PEO was verified by the blue shift of the luminescent peaks. Optically active DNA-wrapped DWNTs within the PEO nanofiber acted as an electrical path as well as an effective reinforcing filler, which dramatically increased the electrical conductivity and mechanical strength of the PEO nanofiber web. Accordingly, our electrically conductive, mechanically tough, DWNT nanofiber web is an interesting multifunctional biomaterial.

AUTHOR INFORMATION

Corresponding Author

*E-mail: yak@endomoribu.shinshu-u.ac.jp.

Notes

The authors declare no competing financial interest.

ACKNOWLEDGMENTS

We acknowledge supports from MEXT grant (Nos. 24810012 and 24310088) and the Research Center for Exotic Nano-Carbon Project, Japan Regional Innovation Strategy Program by the Excellence, JST. J.H.K. acknowledges the support from Nanotechnology Platform Program (Molecule and Material Synthesis) of the Ministry of Education, Culture, Sports, Science and Technology (MEXT), Japan. Y.C.J. acknowledges the support from the KIST Institutional Program, Korea.

ABBREVIATIONS

dsDNA = double-stranded DNA
DWNTs = double-walled carbon nanotubes

REFERENCES

(1) Ramakrishna, S.; Fujihara, K.; Teo, W.-E.; Lim, T.-C.; Ma, Z. *An Introduction to Electrospinning and Nanofibers*; World Scientific, Singapore, 2005.
(2) Agarwal, S.; Greiner, A.; Wendorff, J. H. *Adv. Funct. Mater.* **2009**, *19*, 2863−2879.
(3) Yoshimoto, H.; Shin, Y. M.; Terai, H.; Vacanti, J. P. *Biomaterials* **2003**, *24*, 2077−2082.
(4) Zong, X.; Bien, H.; Chung, C. Y.; Yinc, L.; Fang, D.; Hsiao, B. S. *Biomaterials* **2005**, *26*, 5330−5338.
(5) Zhang, Y.; Venugopal, J. R.; El-Turki, A.; Ramakrishna, S.; Su, B.; Lim, C. *Biomaterials* **2008**, *29*, 4314−4322.
(6) Barnes, C. P.; Sell, S. A.; Boland, E. D.; Simpson, D. G.; Bowlin, G. L. *Adv. Drug Delivery Rev.* **2007**, *59*, 1413−1433.
(7) Agarwal, S.; Wendorff, J. H.; Greiner, A. *Polymer* **2008**, *49*, 5603−5621.
(8) Zhang, Y.; Lim, C. T.; Ramakrishna, S.; Huang, Zh. M. *J. Mater. Sci. Mater. Med.* **2005**, *16*, 933−946.
(9) Kwon, I. K.; Kidoaki, S.; Matsuda, T. *Biomaterials* **2005**, *26*, 3929−3939.
(10) Rho, K. S.; Jeong, L.; Lee, G.; Seo, B. M.; Park, Y. J.; Hong, S. *Biomaterials* **2006**, *27*, 1452−1461.
(11) Tillman, B. W.; Yazdani, S. K.; Lee, S. J.; Geary, R. L.; Atala, A.; Yoo, J. J. *Biomaterials* **2009**, *30*, 583−588.
(12) Roh, J. D.; Nelson, G. N.; Brennam, M. P.; Mirensky, T. L.; Yi, T.; Hazlett, T. F. *Biomaterials* **2008**, *29*, 1454−1463.
(13) Huang, L.; Nagapudi, K.; Apkarian, R. P.; Chaikof, E. *J. Biomater. Sci., Poly. Ed.* **2001**, *12*, 979−993.
(14) Dresselhaus, M. S.; Dresselhaus, G.; Eklund, P. C. *Science of Fullerenes and Carbon Nanotubes*; Academic Press: San Diego, CA, 1996.
(15) Dror, Y.; Salalha, W.; Khalfin, R. L.; Cohen, Y.; Yarin, A. L.; Zussman, E. *Langmuir* **2003**, *19*, 7012−7020.
(16) Salalha, W.; Dror, Y.; Khalfin, R. L.; Cohen, Y.; Yarin, A. L.; Zussman, E. *Langmuir* **2004**, *20*, 9852−9855.
(17) Nakashima, N.; Okuzono, S.; Murakami, H.; Nakai, T.; Yoshikawa, K. *Chem. Lett.* **2003**, *32*, 456−457.
(18) Banerjee, S.; Hemraj-Benny, T.; Wong, S. S. *Adv. Mater.* **2005**, *17*, 17−29.
(19) Zheng, M.; Diner, B. A. *J. Am. Chem. Soc.* **2004**, *126*, 15490−15494.
(20) Fantini, C.; Jorio, A.; Santos, A. P.; Peressinotto, V. S. T.; Pimenta, M. A. *Chem. Phys. Lett.* **2007**, *439*, 138−142.
(21) Zhao, X.; Johnson, J. K. *J. Am. Chem. Soc.* **2007**, *129*, 10438−10445.
(22) Meng, S.; Maragakis, P.; Papaloukas, C.; Kaxiras, E. *Nano Lett.* **2007**, *7*, 45−50.
(23) Chen, Y.; Liu, H.; Ye, T.; Kim, J.; Mao, C. *J. Am. Chem. Soc.* **2007**, *129*, 8696−8697.
(24) Kim, J. H.; Kataoka, M.; Shimamoto, D.; Muramatsu, H.; Jung, Y. C.; Tojo, T.; Hayashi, T.; Kim, Y. A.; Endo, M.; Terrones, M.; Dresselhaus, M. S. *ChemPhysChem* **2009**, *10*, 2414−2417.
(25) Das, D.; Sood, A. K.; Maiti, P. K.; Das, M.; Varadarajan, R.; Rao, C. N. R. *Chem. Phys. Lett.* **2008**, *453*, 266−273.
(26) Tu, X.; Manohar, S.; Jagota, A.; Zheng, M. *Nature* **2009**, *460*, 250−253.
(27) Tu, X.; Hight Walker, A. R.; Khripin, C. Y.; Zheng, M. *J. Am. Chem. Soc.* **2011**, *133*, 12998−13001.
(28) Kim, J. H.; Kataoka, M.; Fujisawa, K.; Tojo, T.; Muramatsu, H.; Vega-Díaz, S.; Tristan-Lopez, F.; Hayashi, T.; Kim, Y. A.; Endo, M.; Terrones, M.; Dresselhaus, M. S. *J. Phys. Chem. B* **2011**, *115*, 14295−14300.
(29) Bellan, L. M.; Cross, J. D.; Strychalski, E. A.; Moran-Mirabal, J.; Craighead, H. G. *Nano Lett.* **2006**, *6*, 2526−2530.
(30) Liu, Y.; Chen, J.; Misoska, V.; Wallace, G. G. *React. Funct. Polym.* **2007**, *67*, 461−467.
(31) Endo, M.; Muramatsu, H.; Hayashi, T.; Kim, Y. A.; Terrones, M.; Dresselhaus, M. S. *Nature* **2005**, *433*, 476.
(32) Kim, Y. A.; Muramatsu, H.; Hayashi, T.; Endo, M.; Terrones, M.; Dresselhaus, M. S. *Chem. Vapor Deposition* **2006**, *12*, 327−330.
(33) Kim, J. H.; Kataoka, M.; Shimamoto, D.; Muramatsu, H.; Jung, Y. C.; Hayashi, T.; Kim, Y. A.; Endo, M.; Park, J. S.; Saito, R.; Terrones, M.; Dresselhaus, M. S. *ACS Nano* **2010**, *4*, 1060−1066.
(34) Bahr, J. L.; Mickelson, E. T.; Bronikowski, M. J.; Smalley, R. E.; Tour, J. M. *Chem. Commun.* **2001**, 193−194.
(35) Muramatsu, H.; Kim, Y. A.; Hayashi, T.; Endo, M.; Yonemoto, A.; Arikai, H.; Okino, F.; Touhara, H. *Chem. Commun.* **2005**, 2002−2004.
(36) Hayashi, T.; Shimamoto, D.; Kim, Y. A.; Muramatsu, H.; Okino, F.; Touhara, H.; Shimada, T.; Miyauchi, Y.; Maruyama, S.; Terrones, M.; Dresselhaus, M. S.; Endo, M. *ACS Nano* **2008**, *2*, 485−488.
(37) Aguiar, A. L.; Barros, E. B.; Capaz, R. B.; Souza Filho, A. G.; Freire, P. T. C.; Mendes Filho, J.; Machon, D.; Caillier, Ch.; Kim, Y. A.; Muramatsu, H.; Endo, M.; San-Miguel, A. *J. Phys. Chem. C* **2011**, *115*, 5378−5384.
(38) Rao, A. M.; Richter, E.; Bandow, S.; Chase, B.; Eklund, P. C.; Williams, K. W.; Menon, M.; Subbaswamy, K. R.; Thess, A.; Smalley, R. E.; Dresselhaus, G.; Dresselhaus, M. S. *Science* **1997**, *275*, 187−191.
(39) O'Connell, M. J.; Bachilo, S. M.; Huffman, C. B.; Moore, V. C.; Strano, M. S.; Haroz, E. H.; Rialon, K. L.; Boul, P. J.; Noon, W. H.; Kittrell, C.; Ma, J.; Hauge, R. H.; Weisman, R. B.; Smalley, R. E. *Science* **2002**, *297*, 593−596.
(40) Cohen, H.; Nogues, C.; Uilien, D.; Daube, S.; Naaman, R.; Porath, D. *Faraday Discuss.* **2006**, *131*, 367.